POLARIMETRIC SAR IMAGE DECOMPOSITION
FOR NON-REFLECTION SYMMETRY CONDITION

Yoshio Yamaguchi*, Motoi Ishido*, Toshifumi Moriyama**, Jian Yang***, Hiroyoshi Yamada*

* Dept. of Information Engineering, Niigata University

Ikarashi 2-8050, Niigata, 950-2181, Japan

yamaguch@ie.niigata-u.ac.jp

** National Institute of Information and Communications Technology

Nukui-Kitamachi 4-2-1, Koganei, Tokyo, 184-8795, Japan

*** Dept. of Electronic Engineering, Tsinghua University

Beijing, 100084 China

1. Introduction

Terrain and land use classification is one of the most important applications of Polarimetric Synthetic Aperture Radar (POLSAR) imaging. A four-component scattering model is proposed to decompose POLSAR images. Covariance matrix approach is used to deal with the non-reflection symmetry scattering case. This scheme includes and extends the three-component decomposition method [1] dealing with the reflection symmetry condition that the co-pol and the cross-pol correlations are close to zero. Circular polarization power term is added as the fourth component to the three component scattering model which describes surface, double bounce, and volume scattering. This circular polarization term is taken into account for the co-pol and the cross-pol correlations which regularly appear in complex urban area scattering and disappear in natural distributed target scatterer. This term is relevant for describing man-made targets in urban area scattering.

2. Covariance Matrix for the Non-Reflection Symmetry Condition

To derive polarimetric scattering characteristics contained in POLSAR image, it is necessary to evaluate the second order statistics of its scattering matrices. Here, we follow the scheme [1] and present covariance matrix approach to derive a four-component scattering model mathematically. The general covariance matrix is defined as

$$\langle [C] \rangle^{HV} = \begin{bmatrix} \langle |S_{HH}|^2 \rangle & \sqrt{2}\langle S_{HH}S_{HV}^* \rangle & \langle S_{HH}S_{VV}^* \rangle \\ \sqrt{2}\langle S_{HV}S_{HH}^* \rangle & 2\langle |S_{HV}|^2 \rangle & \sqrt{2}\langle S_{HV}S_{VV}^* \rangle \\ \langle S_{VV}S_{HH}^* \rangle & \sqrt{2}\langle S_{VV}S_{HV}^* \rangle & \langle |S_{VV}|^2 \rangle \end{bmatrix} \tag{1}$$

where $<\,>$ denotes the ensemble average in the data processing: and the superscript * denotes complex conjugation. Under the non-reflection symmetry condition, $\langle S_{HH}S_{HV}^* \rangle \neq 0$ and $\langle S_{VV}S_{HV}^* \rangle \neq 0$, we have all non-zero terms. Since most of the works have been dealing with the reflection symmetry condition, $\langle S_{HH}S_{HV}^* \rangle \approx \langle S_{VV}S_{HV}^* \rangle \approx 0$, we have to develop the corresponding scattering term. The basic scattering mechanism related to the non-reflection condition is found to be helicity (or equivalently, circular polarization state) of which covariance form is given as

$$\langle [C] \rangle^{hv}_{r-helix} = \frac{1}{4}\begin{bmatrix} 1 & j\sqrt{2} & -1 \\ -j\sqrt{2} & 2 & j\sqrt{2} \\ -1 & -j\sqrt{2} & 1 \end{bmatrix} \quad \text{or} \quad \langle [C] \rangle^{hv}_{l-helix} = \frac{1}{4}\begin{bmatrix} 1 & -j\sqrt{2} & -1 \\ j\sqrt{2} & 2 & -j\sqrt{2} \\ -1 & j\sqrt{2} & 1 \end{bmatrix} \tag{2}$$

This helix (circular polarization) term is assigned to the fourth component of scattering mechanism. Since the Trace of <[C]> is unity, the corresponding power can be given by taking average of a measured covariance matrix as

$$\frac{f_c}{4} = \frac{1}{2}|\text{Im}\{\langle S_{HH}S_{HV}^* \rangle + \langle S_{HV}S_{VV}^* \rangle\}| \tag{3}$$

where f_c is the coefficient to the unit power. The scattering power is based on the trace of covariance matrix which follows.

3. Four-Component Scattering Power Decomposition

We expand the measured covariance matrix using a four scattering model, namely, surface scattering, double bounce scattering, volume scattering, and the circular polarization power term as follows:

$$\langle [C] \rangle^{HV} = f_s \langle [C] \rangle_{surface}^{hv} + f_d \langle [C] \rangle_{double}^{hv} + f_v \langle [C] \rangle_{vol}^{hv} + f_c \langle [C] \rangle_{circular}^{hv}$$

$$= f_s \begin{bmatrix} |\beta|^2 & 0 & \beta \\ 0 & 0 & 0 \\ \beta^* & 0 & 1 \end{bmatrix} + f_d \begin{bmatrix} |\alpha|^2 & 0 & \alpha \\ 0 & 0 & 0 \\ \alpha^* & 0 & 1 \end{bmatrix} + \langle [C] \rangle_{vol}^{hv} + \frac{f_c}{4} \begin{bmatrix} 1 & \pm j\sqrt{2} & -1 \\ \mp j\sqrt{2} & 2 & \pm j\sqrt{2} \\ -1 & \mp j\sqrt{2} & 1 \end{bmatrix} \quad (4)$$

where the first and the second terms are identical with those in [1]. For the third term, $\langle [C] \rangle_{vol}^{hv}$, we choose one of the following covariance matrices according to the relative measurement value of $\langle |S_{HH}|^2 \rangle$ and $\langle |S_{VV}|^2 \rangle$.

$$\langle [C] \rangle_{vol}^{hv} = \frac{1}{15}\begin{bmatrix} 8 & 0 & 2 \\ 0 & 4 & 0 \\ 2 & 0 & 3 \end{bmatrix}, \qquad \langle [C] \rangle_{vol}^{hv} = \frac{1}{8}\begin{bmatrix} 3 & 0 & 1 \\ 0 & 2 & 0 \\ 1 & 0 & 3 \end{bmatrix}, \qquad \langle [C] \rangle_{vol}^{hv} = \frac{1}{15}\begin{bmatrix} 3 & 0 & 2 \\ 0 & 4 & 0 \\ 2 & 0 & 8 \end{bmatrix} \quad (5)$$

These matrices are derived by the second order statistics for randomly oriented wires with appropriate probability density functions considering actual tree distribution. This choice allows us to make a straightforward best-fit to the measured data $\langle |s_{HH}|^2 \rangle \neq \langle |s_{VV}|^2 \rangle$.

Comparing the matrix elements yields the following 5 equations with 6 unknowns $\alpha, \beta, f_s, f_d, f_v$ and f_c

$$\langle |S_{HH}|^2 \rangle = f_s |\beta|^2 + f_d |\alpha|^2 + \frac{8}{15}f_v + \frac{f_c}{4} \quad (6a) \qquad \langle |S_{HV}|^2 \rangle = \frac{2}{15}f_v + \frac{f_c}{4} \quad (6b)$$

$$\langle |S_{VV}|^2 \rangle = f_s + f_d + \frac{3}{15}f_v + \frac{f_c}{4} \quad (6c) \qquad \langle S_{HH}S_{VV}^* \rangle = f_s\beta + f_d\alpha + \frac{2}{15}f_v - \frac{f_c}{4} \quad (6d)$$

$$\frac{1}{2}\left\{ \langle S_{HH}S_{HV}^* \rangle + \langle S_{HV}S_{VV}^* \rangle \right\} = j\frac{f_c}{4}. \quad (6e)$$

Since the left hand side of (6) is a measurable quantity, we can determine f_c directly with the aid of (3).

$$f_c = P_c = 2 \left| \mathrm{Im}\left\{ \langle S_{HH}S_{HV}^* \rangle + \langle S_{HV}S_{VV}^* \rangle \right\} \right| = 2 \left| \mathrm{Im}\left\langle S_{HV}^* \left(S_{HH} - S_{VV} \right) \right\rangle \right| \quad (7)$$

Then, (6b) gives the volume scattering coefficient f_v directly as

$$f_v = \frac{15}{2}\left(\langle |S_{HV}|^2 \rangle - \frac{f_c}{4} \right) \quad (8)$$

The remaining 4 unknowns with 3 equations can be obtained in the same manner as shown in [1]. The scattering powers, *Ps, Pd, Pv*, and *Pc*, corresponding to surface, double bounce, volume, and circular polarization contributions, respectively, are obtained as

$$P_s = f_s\left(1 + |\beta|^2\right), \quad P_d = f_d\left(1 + |\alpha|^2\right), \quad P_v = f_v, \quad P_c = f_c \quad (9)$$

$$P_t = P_s + P_d + P_v + P_c = \langle |S_{HH}|^2 + 2|S_{HV}|^2 + |S_{VV}|^2 \rangle. \quad (10)$$

The above equations (5)-(10) are the main set of expressions for the four-component decomposition.

4. Algorithm for Decomposition

When we apply the four component decomposition scheme to POLSAR data directly, we sometimes encounter a problem in that the coefficients f_s or f_d become negative for certain areas.

Since the negative coefficient indicates the corresponding power is negative, it is inconsistent with the physical phenomenon. A typical feature of such areas is that $\langle | S_{HV} |^2 \rangle$ is rather predominant compared to $\langle | S_{HH} |^2 \rangle$ and to $\langle | S_{VV} |^2 \rangle$. These areas reside within small sections of geometrically complicated man-made scattering (cultivated) and of forested areas. In order to avoid such inconsistency, we devised an algorithm for the four-component decomposition which could be applied to general POLSAR data image analyses.

The main point for avoiding the inconsistency is to use the following power ratio:

$$2 \langle | S_{HV} |^2 \rangle : \langle | S_{HH} |^2 \rangle \ or \ \langle | S_{VV} |^2 \rangle \tag{11}$$

based on statistics [3]-[4] and on our experiences of POLSAR image analysis [5]. The theoretical studies showed that co-pol radar channel power and cross-pol channel power are of the magnitude ratio of 2:1 statistically [3]-[4]. This condition is used in the middle stage of the four-component decomposition algorithm in Fig.1
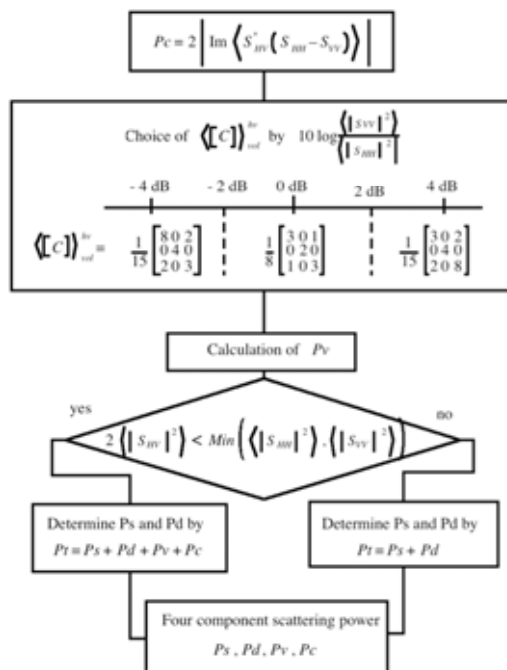

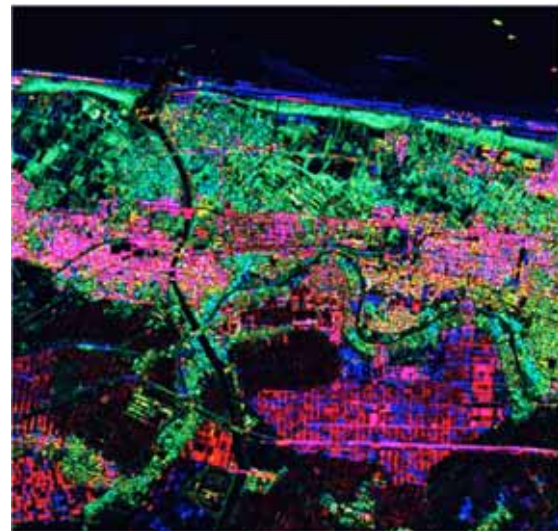Fig.1 Algorithm for the four component scattering power decomposition

Fig.2 Decomposed image of Niigata University area Ps (blue), Pd (red), and Pv (green),

5. Example

An L-band Pi-SAR data set was used for the four-component decomposition. The Pi-SAR sensor is an airborne POLSAR system developed by the former Communications Research Laboratory (now NICT) and NASDA (now JAXA) of Japan. The resolution in the L-band image is 3 m by 3 m. The area chosen for analysis is Niigata-city, Japan, which includes an urban area, a river, and paddy rice fields. A color image of Niigata University area is shown in Fig.2 resulted from the four component decomposition with Ps (blue), Pd (red), and Pv (green) . The decomposed result seems acceptable from the view point of electromagnetic scattering phenomena.

In order to verify the decomposed result, we picked up a small area to see the details of the decomposed image. Fig.3 shows a zoomed-up image nearby a river in Niigata city. The image (a) is an aerial photo, (b) is three component contribution color image, and (c) shows overlay image where the circular polarization power generates. It is seen that the double bounce power Pd is strong at bridges due to water-bridge reflections. Also we can see strong Pd from buildings whose facets are parallel to

SAR flight path. On the other hand, buildings whose facets are not parallel to SAR flight path exhibit green color (volume scattering mainly caused by the cross polarized component (8)). Vegetation area is identified by *Pv* correctly. The fourth component, *Pc*, is generated from complex man-made structures and facets of buildings.
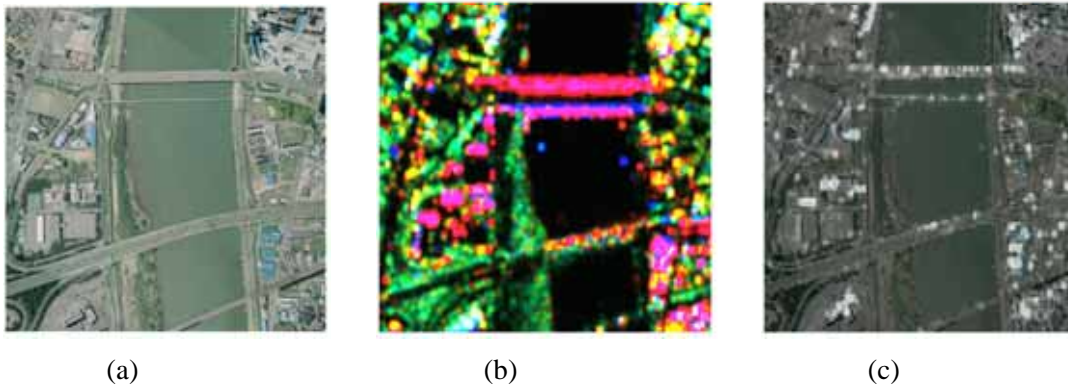

<div align="center">(a)   (b)   (c)</div>

Fig.3 Four component decomposed image near Shinano river in Niigata city.

(a) A photo. (b) *Ps* (blue), *Pd* (red), and *Pv* (green), (c) Overlay image of *Pc* to (a).

6. Conclusion

A four-component scattering model based on the covariance matrix is presented for polarimetric SAR data decomposition. The four components are single bounce, double bounce, volume scattering and circular polarization powers. The decomposition scheme incorporates non-reflection symmetry condition which has not been dealt with. The fourth component, circular polarization power, corresponds to the imaginary part of $\langle S_{HH} S_{HV}^* \rangle$ which often appears in complex urban area and disappears in natural distributed target. The volume scattering symmetric and asymmetric covariance can be chosen to fit the relative magnitude between $\langle |S_{HH}|^2 \rangle$ and $\langle |S_{VV}|^2 \rangle$ of measurement data. An algorithm is developed taking account of physical statistics. The decomposed result is demonstrated with L-band Pi-SAR image of Niigata city, Japan.

References

[1] A. Freeman and S. L. Durden, "A three-component scattering model for polarimetric SAR data," *IEEE Trans. Geoscience Remote Sensing*, vol.36, no.3, pp.963-973, 1998
[2] S. R. Cloude and E. Pottier, "A review of target decomposition theorems in radar polarimetry," *IEEE Trans. Geoscience Remote Sensing,* vol.34, no.2, pp.498-518, 1996
[3] Y. Ke, "Notes on invariant characters of radar cross sections," *2001 CIE Int'l Conference on Radar Proc.*, pp.418-422, 2001.
[4] Jian Yang, Ph.D dissertation, "On theoretical problems in radar polarimetry," Graduate School of Science and Technology, Niigata University, Japan, 2000.
[5] Y. Yamaguchi, T. Moriyama, M. Ishido, H. Yamada, "Four Component Scattering Model for Polarimetric SAR Image Decomposition," Proc. of 2004 Korea-Japan Joint Conference on AP/EMC/EMT, pp.105-108, Nov.22-23, 2004